Periodic charge-density modulations on graphite near platinum particles

J. Xhie, K. Sattler, U. Müller, N. Venkateswaran, and G. Raina
Department of Physics and Astronomy, University of Hawaii at Manoa, Honolulu, Hawaii 96822
(Received 26 June 1990; revised manuscript received 19 October 1990)

We have imaged ten different superstructures on highly oriented pyrolytic graphite near adsorbed platinum particles using a scanning tunneling microscope. These superstructures are localized in small areas near the platinum particles and decay within a distance of 2–5 nm into the graphite lattice. When Fourier transformed, the observed structures contain up to three pairs of first-order Fourier components in addition to those of graphite. These Fourier components have different intensities and phases in different directions, but they have the same period of $1.5a$ (a is the lattice constant of graphite) and are rotated 30° relative to the graphite lattice. We show that the observed features are mainly due to a periodic charge-density modulation superimposed onto the graphite lattice, i.e., the platinum particles perturb the surface charge density of graphite giving rise to the superstructures in the nearby regions.

INTRODUCTION

Recently, superstructures on graphite near defects have been reported.[1–5] The defects can be steps, holes in the graphite lattice, or adsorbed molecules. The superstructures have been found to have a periodicity of $(\sqrt{3}\times\sqrt{3})R30°$ and decay over a distance of a few nanometers. Mizes and Foster[4] have proposed an electronic-perturbation model for such structures near isolated adsorbed molecules. They suggest that the adsorbed molecules perturb the surface charge density of graphite giving periodic oscillations similar to Friedel oscillations. The oscillations have a periodicity $\sqrt{3}$ times the graphite lattice constant, and the symmetry of the oscillations reflects the nature of the defect. Nakagawa *et al.*[5] have observed similar structures near a step. Besides the $(\sqrt{3}\times\sqrt{3})R30°$ periodicity, they find that in a unit cell of the $\sqrt{3}\times\sqrt{3}$ structure the three β-site atoms show different brightness. Close to the step they observe an apparent horizontal displacement of graphite atoms and a so-called "triplet" structure. They ascribe the observed features to an interference of electron waves scattered at the step. It successfully explained the $(\sqrt{3}\times\sqrt{3})R30°$ periodicity, the brightness difference, and the decay with distance, but could not explain the apparent horizontal displacement of the graphite atoms and the "triplet" structure.

Although various scanning tunnel microscope (STM) images of clean graphite have been reported,[6] the superstructures which have a periodicity of $(\sqrt{3}\times\sqrt{3})R30°$ are completely different and are found only near defects on graphite. This suggests that they are induced by a perturbation caused by surface defects. However, it is still unclear how the defects influence the nearby graphite lattice. The electronic-perturbation model by Mizes and Foster[4] and the electron-wave-interference model by Nakagawa *et al.*[5] explain only some of the features. To fully understand the physics of these superstructures, one needs more experimental data and more theoretical analyses.

In this paper we show a variety of superstructures of graphite found near adsorbed platinum particles. We show that the observed features are mainly due to an electronic effect which can be described by a superposition of the graphite lattice and a periodic modulation of the surface charge density localized in the surrounding regions of the platinum particles.

EXPERIMENT

The experiments were performed at room temperature using a scanning tunneling microscope[7] in air. All the images presented here were taken in constant current mode where the tip-sample distance was kept constant and the variation of the z motion of the tip was recorded.

The samples were prepared in a high vacuum (10^{-7} Torr) chamber by vapor deposition of platinum on fresh-

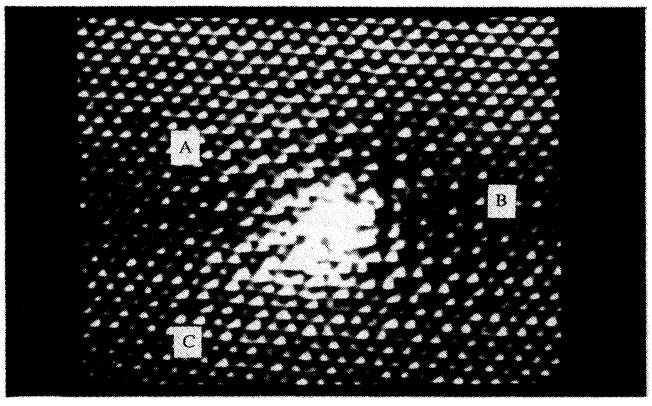

FIG. 1. STM image of a platinum particle adsorbed on graphite. The particle appears as the bright area in the center and has a size of about 0.8 nm. Around the particle there are regions of graphite forming superstructures as indicated by A, B, C.

ly cleaved graphite substrates. A small strip of platinum wrapped on a tungsten filament was placed about 10 cm away from the substrate and a current of 45 A was applied to the filament. A few seconds after the platinum started evaporating, we turned off the current so that only a small amount of platinum was deposited onto the substrate. After deposition, the sample was analyzed by x-ray photoelectron spectroscopy (XPS), which showed a coverage of 2–4% of a platinum monolayer on the graphite surface.

The sample was then transferred to the STM operating at atmospheric conditions. The STM images were taken at constant current mode with positive tip bias voltages of 3–160 mV and tunneling currents of 1.5–14.0 nA. At large scales (100–440 nm) we imaged platinum particles of sizes of 0.8–2.5 nm randomly distributed on the graphite surface. The particles were stable for at least a week although our STM images presented in this paper were taken within two days after the sample was exposed to air. We have investigated five different samples prepared in the same way and all of them showed the same superstructures.

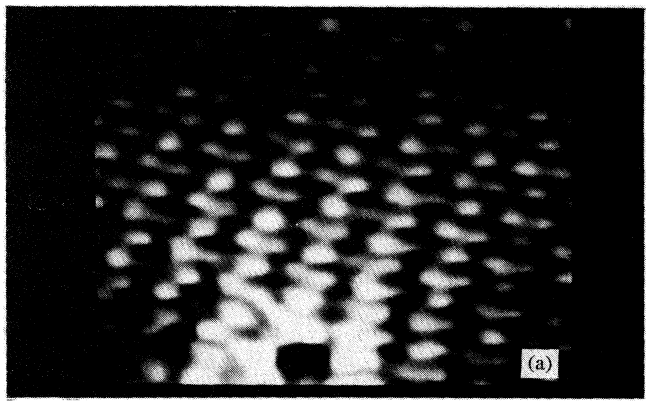

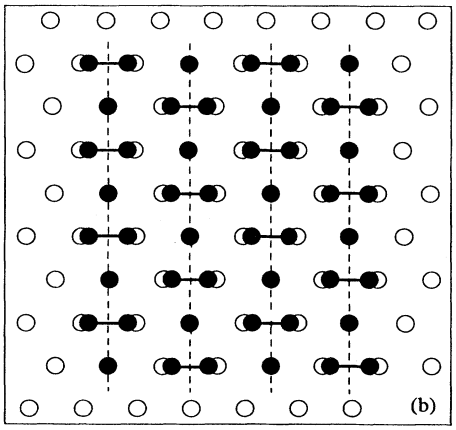

FIG. 2. (a) STM image of a superstructure with the PCDM in one direction on the triangular graphite lattice. (b) Schematic model corresponding to the superstructure in (a). The open circles represent the positions of the carbon atoms in the undisturbed triangular graphite lattice. The solid circles represent the positions of the bright spots in the STM image. The first-order Fourier component corresponding to the superstructure and the maxima of the PCDM are shown as dashed lines.

RESULTS AND DISCUSSION

Figure 1 shows a typical grey-scale image of a platinum particle adsorbed on graphite. It appears as the bright area in the center and has a size of about 0.8 nm. Around the particle the graphite lattice appears to be distorted to form different superstructures as shown at the upper left (A), right (B), and lower left (C) of the particle. The intensity of the superstructures decays away from the particle over a distance of 2–3 nm. Similar images of superstructures were obtained many times near different platinum particles and they do not display an obvious dependence on the particle size and shape. The superstructures shown in this paper were reproducible for at least five scans (30 s). Occasionally, the structures changed from one type to another during the process of imaging and in some cases disappeared after some time. These changes in the structures are probably due to slight

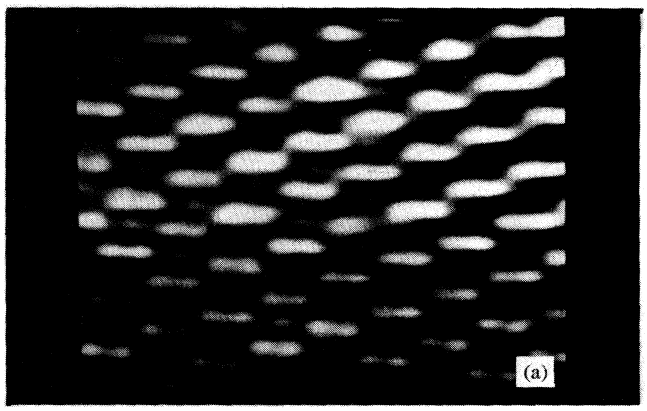

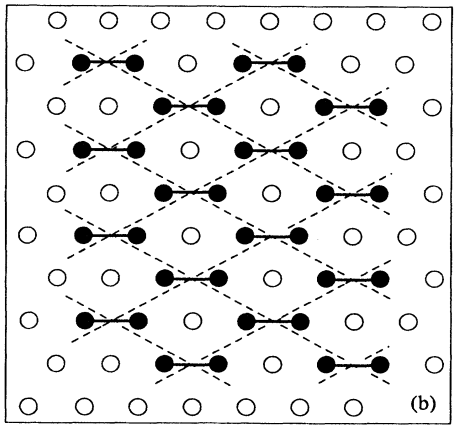

FIG. 3. (a) STM image of a superstructure with the PCDM's in two directions on the triangular graphite lattice. (b) Schematic model.

variations in the bond lengths and orientations of the atoms in the particles[8] which could affect the strain on the substrate and lead to different surface electronic arrangements.

In Figs. 2–11 we show ten different superstructures found near different particles where (a) is the STM top-view image and (b) is the corresponding schematic model. In (b) the open circles represent the positions of the carbon atoms in the undisturbed triangular or hexagonal graphite lattice.[9] The solid circles show the positions of the bright spots in the STM images. For each of the images we performed a two-dimensional Fourier analysis. The first-order Fourier components that correspond to the superstructures are indicated as dashed lines in (b). From the Fourier analysis we can divide the superstructures into three sets with one, two, or three dominant Fourier components. Figure 2 shows a superstructure where one of the Fourier components is dominant and is oriented at an angle of 30° to the graphite lattice. The period of the Fourier components is $1.5a$, where $a=0.245$ nm is the lattice constant of the graphite. Figures 3–6 show four superstructures where two of the Fourier components are dominant. Their directions have an angle of 60° relative to each other and 30° to the graphite lattice. The period of the Fourier components is again $1.5a$. Figures 7–10 show a set of four superstructures. Their Fourier components reveal the same features in periodicity and orientation as the previous ones except that all three Fourier components are comparable and each has an angle of 60° to the other. Also, for all the superstructures that we have analyzed each Fourier component has a phase relative to the graphite lattice and these phases are independent from each other.

Figure 11 shows a special superstructure where one of the two dominant Fourier components has a period of $0.75a$, which is half of the period of the other Fourier components. But its orientation is still 30° rotated relative to the graphite lattice.

The ten superstructures shown in Figs. 2–11, although different in appearance, have many characteristics in common. They are localized in small areas near the platinum particles and decay within a distance of 2–5 nm into the graphite lattice. The Fourier components of these structures always have a period of $1.5a$ (except in the last

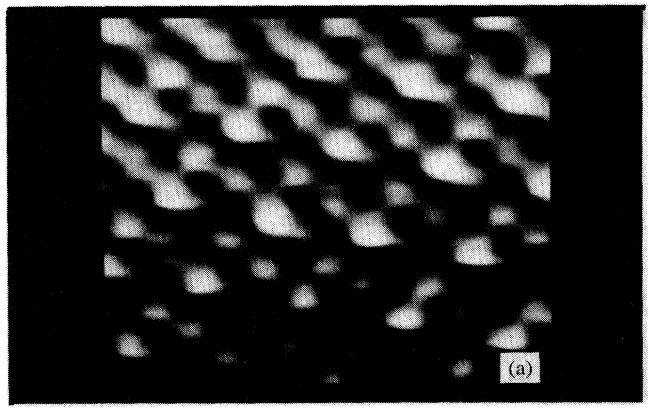

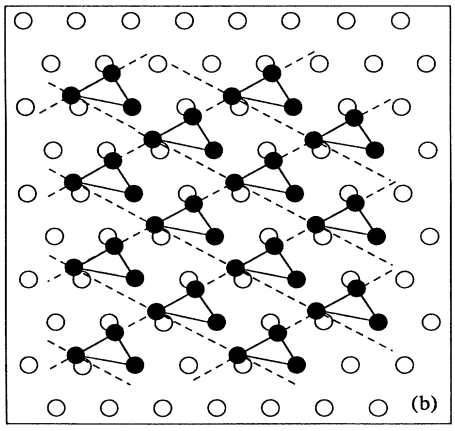

FIG. 4. (a) STM image of a superstructure with the PCDM's in two directions on the triangular graphite lattice but with different phases than in Fig. 3. (b) Schematic model.

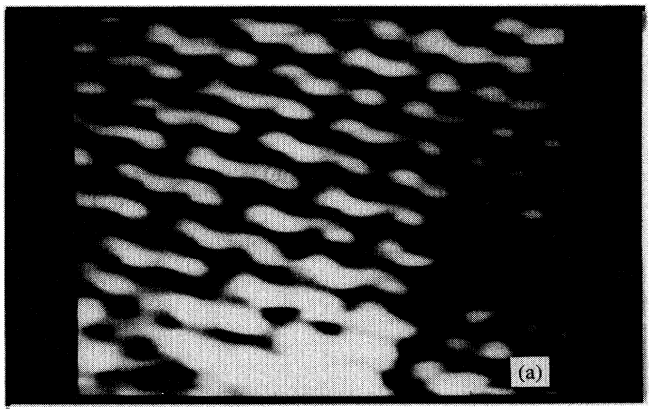

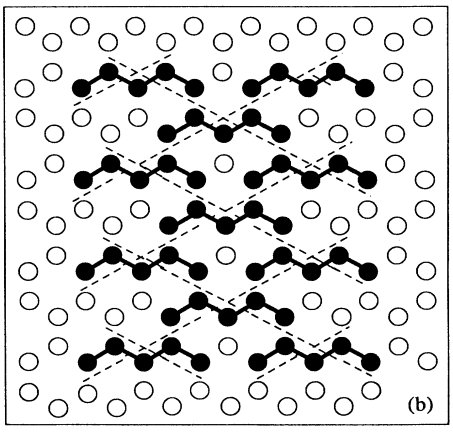

FIG. 5. (a) STM image of a superstructure with the PCDM's in two directions on the hexagonal graphite lattice. (b) Schematic model.

case, $0.75a$) and their orientation is rotated by 30° with respect to the graphite lattice. The period of $1.5a$, as well as the rotation of 30°, corresponds to the second-nearest-neighbor lattice of the triangular graphite lattice (as can be easily seen in Fig. 7).

We exclude the possibility that the superstructures are due to multiple-tip effects because (i) the superstructures have been found only near the platinum particles but never on plain graphite, and (ii) different superstructures have been imaged using the same tip and even within the same scan lines, as seen in Fig. 1 where regions A and B are scanned alternatively from right to left.

We also exclude the possibility that the superstructures are only due to an atomic reconstruction of the graphite lattice. Figure 12(a) shows a STM image of a superstructure analogous to the one in Fig. 2(a). Figure 12(b) shows a section taken along the line AB as indicated in Fig. 12(a). Going from right to left, the section curve shows first the atomic corrugation of the graphite atoms at β sites and then the corrugation of the superstructure. The arrow indicates the position where the peaks of two graphite atoms begin to grow together and become one peak. From thereon, every other peak is actually positioned over two graphite atoms as indicated by the solid circles. Since the two carbon atoms cannot be that close, the bright spots that form the superlattice do not represent the real positions of the graphite atoms. Therefore, the observed superstructures are not a real picture of a possible surface atomic reconstruction of the graphite lattice but are due to a periodic modulation of the surface charge density.

To further understand the physics of the superstructures, one has to take into account the detailed features of all the observed structures. We ascribe these structures to a superposition of the graphite lattice and a localized periodic charge-density modulation (PCDM). This model explains all the features we have observed. As shown in Figs. 2(b)–11(b), the dashed lines that were used to represent the Fourier components of the superstructures can now be used to represent the maxima of the PCDM. They have a period of $1.5a$ (except in the last case, $0.75a$) and are oriented in the three symmetry directions, each rotated 30° to the graphite lattice.

Due to the periodic charge-density modulation, the un-

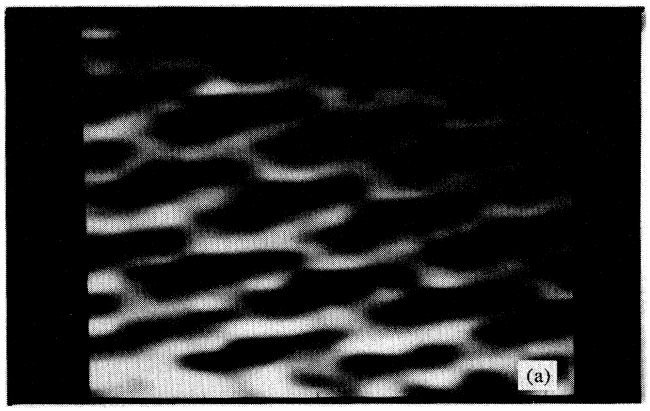

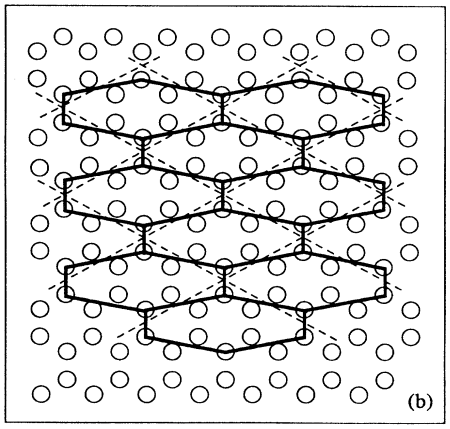

FIG. 6. (a) STM image of a superstructure with the PCDM's in two directions on the hexagonal graphite lattice but with different phases than in Fig. 5. (b) Schematic model.

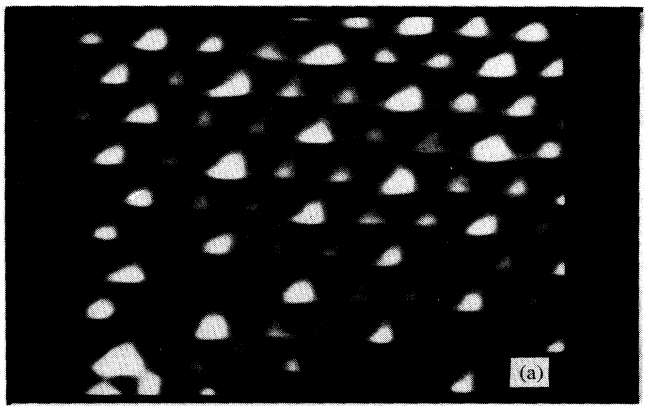

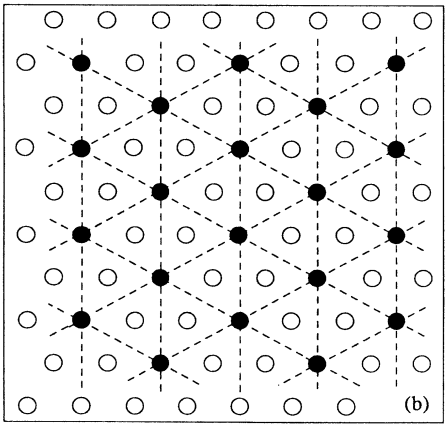

FIG. 7. (a) STM image of a superstructure with the PCDM's in three directions on the triangular graphite lattice. (b) Schematic model.

derlying graphite atoms appear to be either highlighted if the maxima sit right on the atoms or otherwise shifted toward the maxima. For example, the superstructure in Fig. 2 is formed by the modulation in only one direction. Therefore, the graphite atoms appear to form a line-pattern structure. Similar arguments are also applicable to the superstructures in Figs. 3–11 where the periodic charge-density modulations exist in two or three directions. The different superstructures are formed by the combination of the underlying graphite lattice, either triangular or hexagonal, and the periodic charge-density modulation in one, two, or three directions, each with its own intensity and phase.

The difference in the intensities of the periodic charge-density modulation sometimes gives rise to small apparent rotations of the unit cells of the superstructure. Figure 13(a) shows a STM image where the superstructure is similar to that of Fig. 3. It is formed by two PCDM's with their vertices sitting on the bridge sites of the graphite lattice. Therefore, the atoms next to the vertices are highlighted and appear as dimers. Along the line indicated in Fig. 13(a), the orientation of the dimers gradually changes from the lower part to the upper part of the image. At the lower part of the image the dimers are aligned along the graphite orientation. But when going to the upper part, the dimers rotate gradually relative to the graphite lattice up to a maximum rotation of 15°. This gradual dimer rotation can be explained by the different intensities and different decay rates of the PCDM's in the two directions. As shown in Fig. 13(b), when the modulation in one direction is stronger than in the other, the position of the atoms seems to be shifted toward the stronger modulation so that the dimers appear to be rotated. This rotation also decays gradually with the distance from the particle.

In Fig. 8(a) the superstructure shows a regular brightness difference of the white spots in a unit cell of the superlattice. The same "brightness difference" was also observed by Nakagawa *et al.*[5] With our PCDM model it can be easily produced by a small phase shift of the

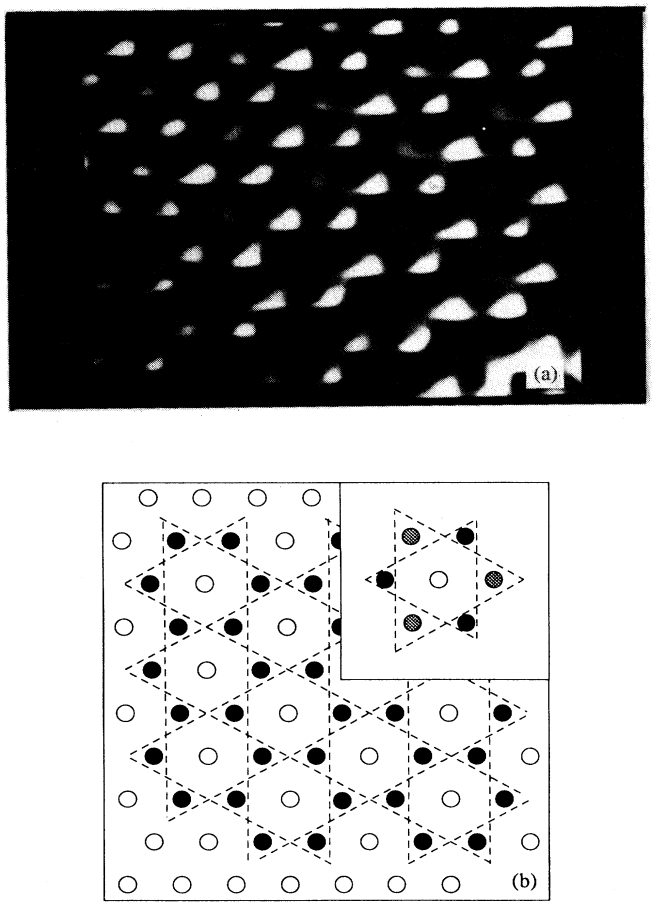

FIG. 8. (a) STM image of a superstructure with the PCDM's in three directions on the triangular graphite lattice but with different phases than in Fig. 7. (b) Schematic model. The inset shows the model of the brightness difference observed in (a).

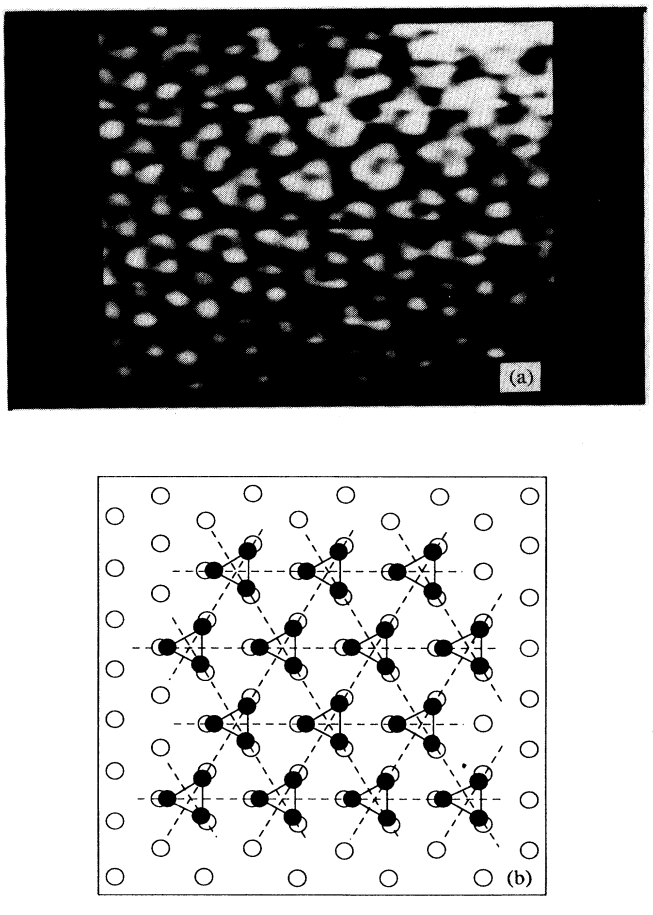

FIG. 9. (a) STM image of a superstructure with the PCDM's in three directions on the triangular graphite lattice but with different phases than in Figs. 7 and 8. (b) Schematic model.

modulation in all three directions, as shown in the inset of Fig. 8(b). Therefore, in a hexagon of the superlattice, three of the outer atoms are highlighted most, and the other three are highlighted less, but are still more highlighted than the center atom.

Because of the many possibilities of superimposing the underlying graphite lattice, either triangular or hexagonal, with the dominant periodic charge-density modulations of various intensities and phases, we expect that more types of superstructures near defects may be found in the future.

It is worth mentioning here that for other metal clusters, such as silver and gold adsorbed on graphite, similar superstructures have been observed previously both in air and in ultrahigh vacuum.[10]

Although the PCDM model explains almost all the observed features, it is still a phenomenological description. The origin of the PCDM's might be explained in the framework of charge-density waves (CDW) in conjunction with periodic lattice distortions (PLD), phenomena observed for various quasi-two-dimensional layered materials. CDW's are caused by the instability of the Fermi surface and have been studied by STM for many transition-metal dichalcogenides.[11] Recently, various CDW vertex structures were found for $TaSe_2$ and could be explained by a phase-shift procedure,[12] similar to the one used in this paper. It involves different lock-in positions for periodic charge-density lattices relative to the underlying atomic lattice. However, such metastability of a CDW, as well as its periodicity and orientation, has not yet been explained theoretically.

CONCLUSION

The observed superstructures found near platinum particles on highly oriented pyrolytic graphite are due to the superposition of the periodic charge-density modulations with the underlying graphite lattice. These periodic charge-density modulations are localized in small areas near the platinum particles, or generally near defects, on graphite and decay as the distance from the particles increases. They have the same period of $1.5a$ (except in one case, $0.75a$) and exist in three possible directions, each rotated 30° relative to the graphite lattice. The image of the

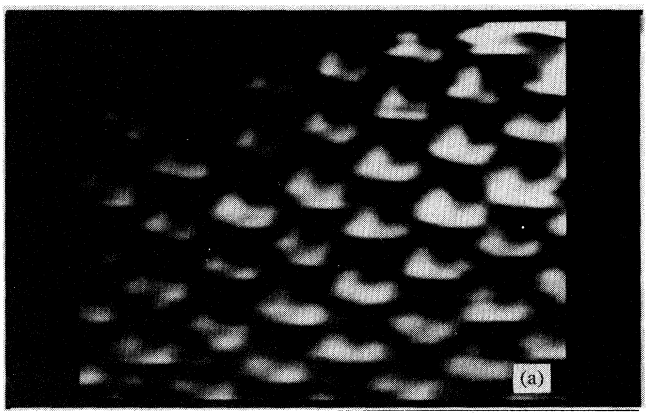

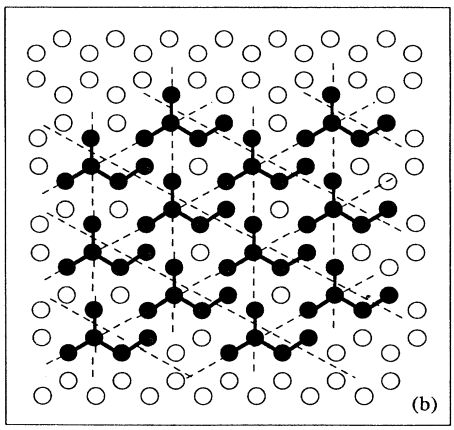

FIG. 10. (a) STM image of a superstructure with the PCDM's in three directions on the hexagonal graphite lattice. (b) Schematic model.

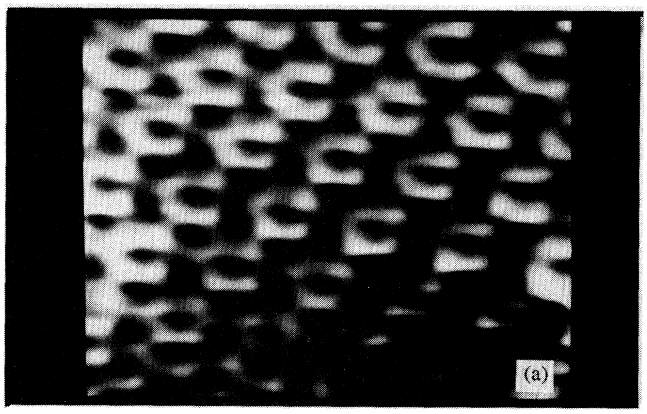

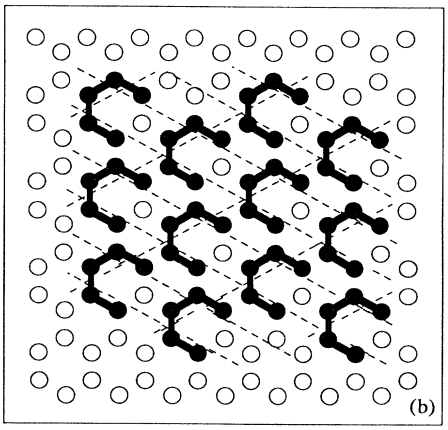

FIG. 11. (a) STM image of a special superstructure with the PCDM's in two directions on the hexagonal graphite lattice. The PCDM in one of the directions has a period of $0.75a$, which is half of the period of the other PCDM's. (b) Schematic model.

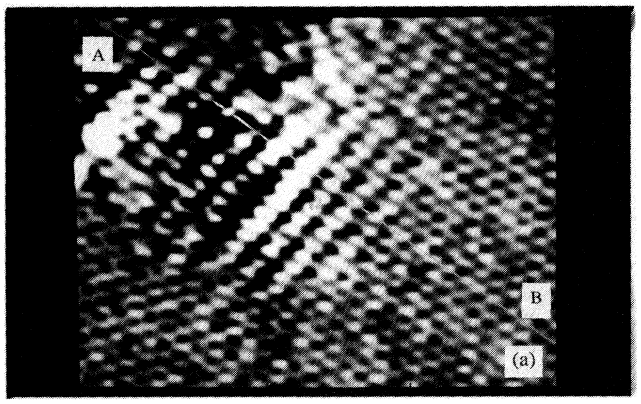

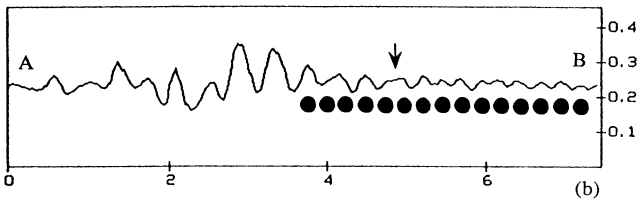

FIG. 12. (a) STM image of a superstructure analogous to the one in Fig. 2. (b) A section taken along the line AB as indicated in (a). The solid circles represent the positions of the underlying graphite atoms at β sites. The arrow indicates the position where the peaks of two graphite atoms begin to grow together.

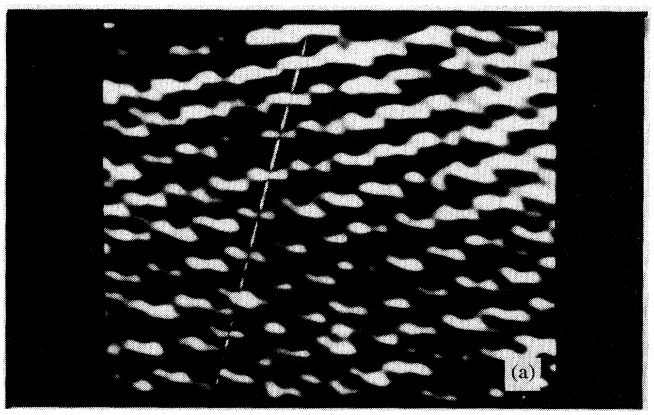

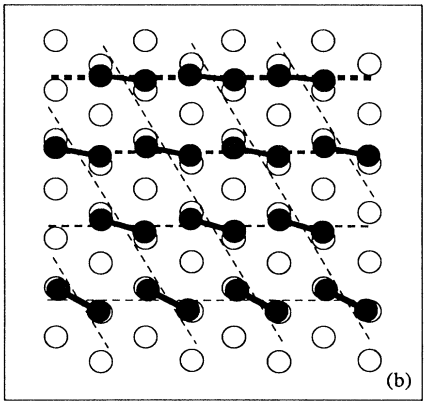

FIG. 13. (a) STM image of a superstructure similar to the one in Fig. 3. The orientation of the dimers along the line changes gradually from the lower part to the upper part. (b) Schematic model of the superstructure in (a) showing the gradual rotation of the dimers. The dashed lines represent the maxima of the PCDM's and their thickness is proportional to the intensity of the PCDM.

superstructures depends on the dominant periodic charge-density modulations and their relative intensities and phases.

ACKNOWLEDGMENTS

We are indebted to W. Pong and J. F. Zheng, who prepared some of the samples. We gratefully acknowledge discussions with P. Lam and B. Kaiser. We thank M. Matsunaga and R. Tom for technical assistance. U.M. acknowledges support from the Swiss National Foundation and J.X. acknowledges support from the Research Corporation of the University of Hawaii. This work was supported by the Project Development Fund of the University of Hawaii, by the Hawaii Natural Energy Institute, and by the New Energy Development Organization, Japan.

[1]Phys. Today, **41**, 129 (1988).
[2]T. R. Albrecht, H. A. Mizes, J. Nogami, S. -I. Park, and C. F. Quate, Appl. Phys. Lett. **52**, 362 (1988).
[3]J. P. Rabe, M. Sano, D. Batchelder, and A. A. Kalatchev, J. Microsc. (Oxford) **152**, 573 (1988).
[4]H. A. Mizes and J. S. Foster, Science **244**, 559 (1989).
[5]Y. Nakagawa, H. Bando, M. Ono, and K. Kajimura (unpublished).
[6]H. A. Mizes, S. -I. Park, and W. A. Harrison, Phys. Rev. B **36**, 4491 (1987).
[7]Digital Instruments, Inc., Santa Barbara, CA.
[8]E. Ganz, K. Sattler, and J. Clarke, Phys. Rev. Lett. **18**, 1856 (1988).
[9]D. Tomanek, S. Louie, H. J. Mamin, D. W. Abraham, R. E. Thomson, E. Ganz, and J. Clarke, Phys. Rev. B **35**, 7790 (1987).
[10]E. Ganz, K. Sattler, and J. Clarke (unpublished).
[11]R. V. Coleman, B. Giambattista, P. K. Hansma, A. Johnson, W. W. McNairy, and C. G. Slough, Adv. Phys. **37**, 559 (1988).
[12]G. Raina, K. Sattler, U. Müller, N. Venkateswaran, and J. Xhie, J. Vac. Sci. Technol. B (to be published).

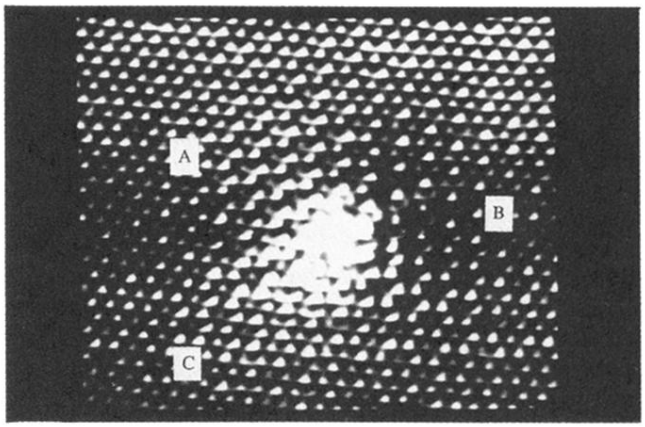

FIG. 1. STM image of a platinum particle adsorbed on graphite. The particle appears as the bright area in the center and has a size of about 0.8 nm. Around the particle there are regions of graphite forming superstructures as indicated by A, B, C.

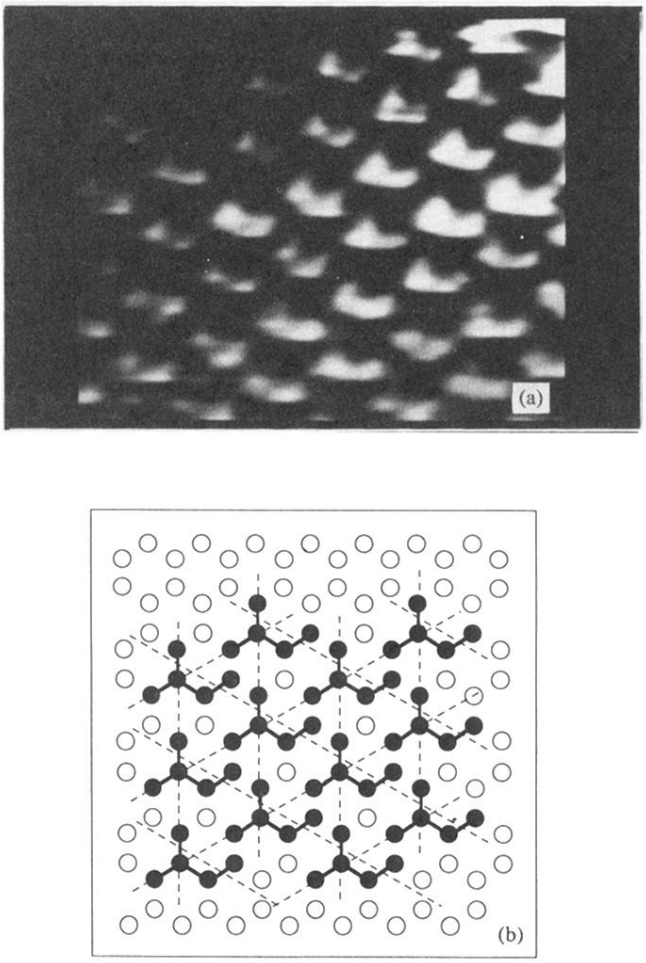

FIG. 10. (a) STM image of a superstructure with the PCDM's in three directions on the hexagonal graphite lattice. (b) Schematic model.

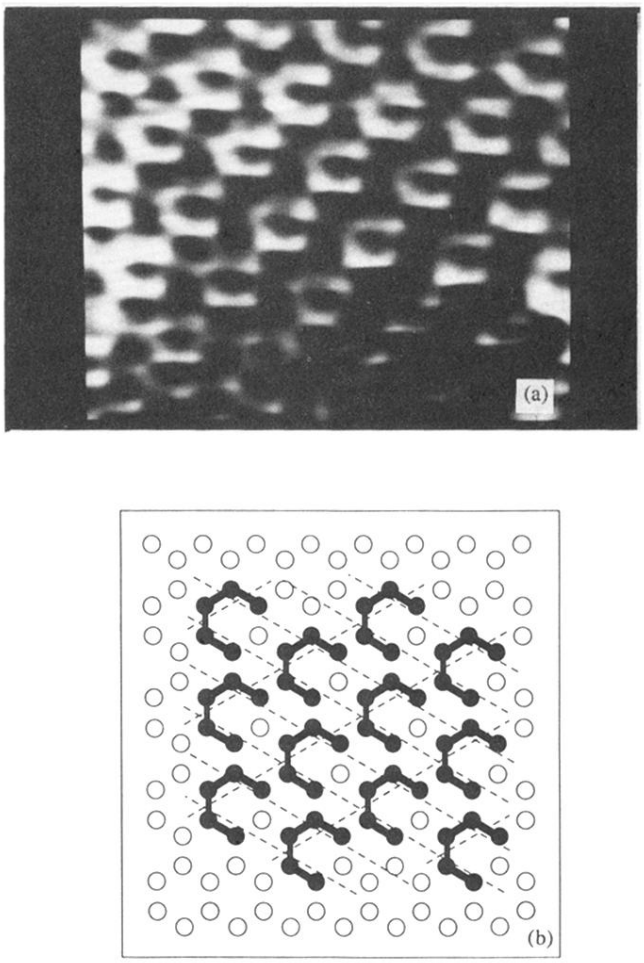

FIG. 11. (a) STM image of a special superstructure with the PCDM's in two directions on the hexagonal graphite lattice. The PCDM in one of the directions has a period of $0.75a$, which is half of the period of the other PCDM's. (b) Schematic model.

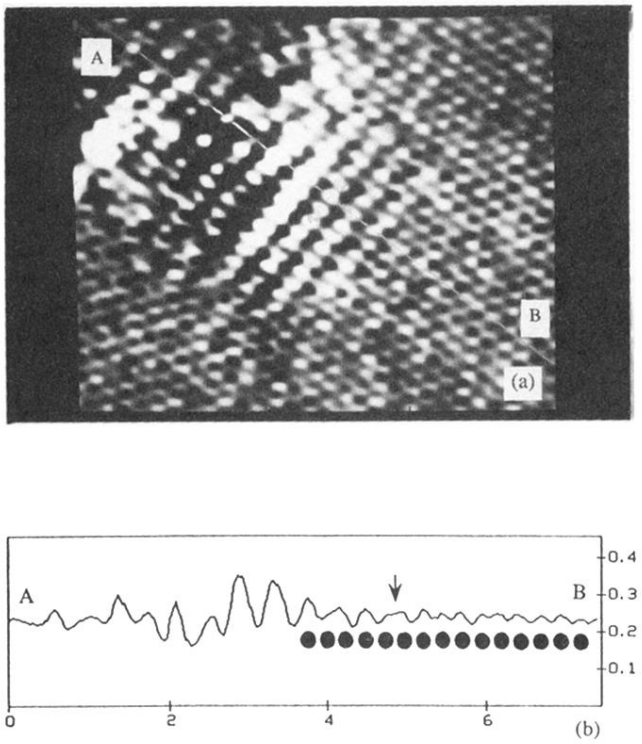

FIG. 12. (a) STM image of a superstructure analogous to the one in Fig. 2. (b) A section taken along the line AB as indicated in (a). The solid circles represent the positions of the underlying graphite atoms at β sites. The arrow indicates the position where the peaks of two graphite atoms begin to grow together.

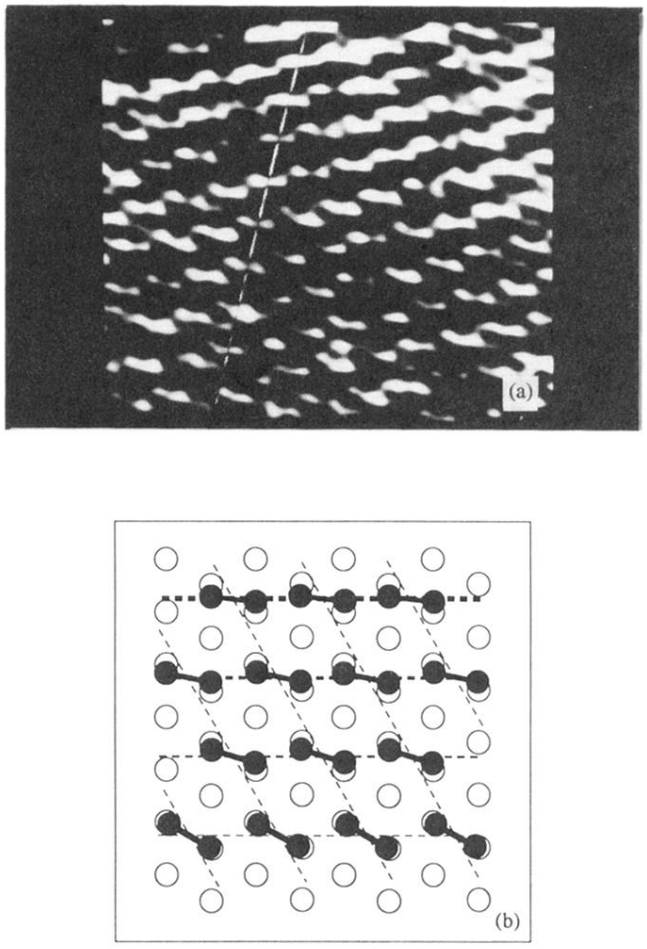

FIG. 13. (a) STM image of a superstructure similar to the one in Fig. 3. The orientation of the dimers along the line changes gradually from the lower part to the upper part. (b) Schematic model of the superstructure in (a) showing the gradual rotation of the dimers. The dashed lines represent the maxima of the PCDM's and their thickness is proportional to the intensity of the PCDM.

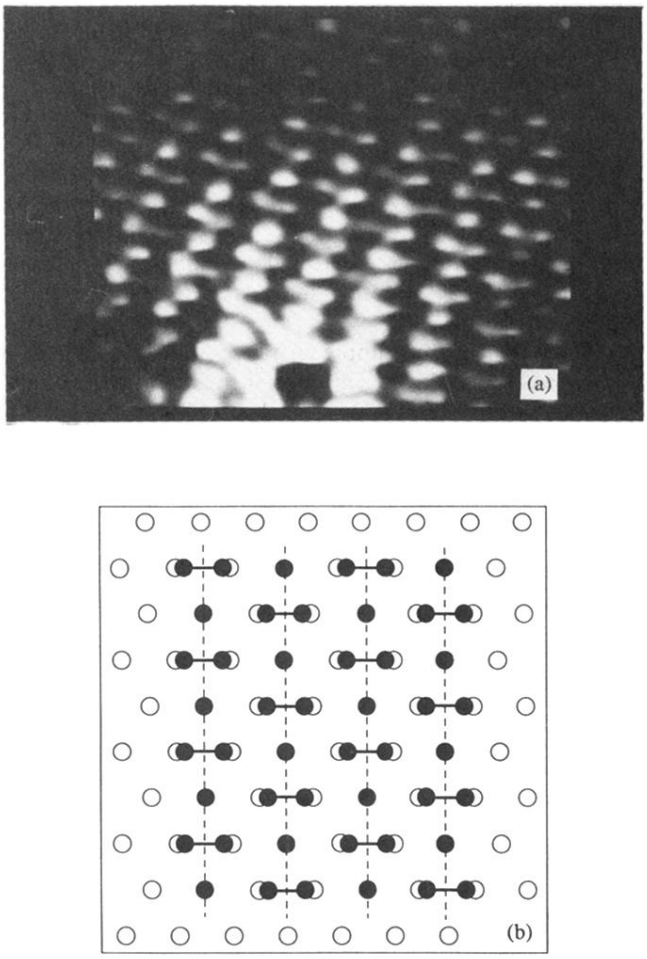

FIG. 2. (a) STM image of a superstructure with the PCDM in one direction on the triangular graphite lattice. (b) Schematic model corresponding to the superstructure in (a). The open circles represent the positions of the carbon atoms in the undisturbed triangular graphite lattice. The solid circles represent the positions of the bright spots in the STM image. The first-order Fourier component corresponding to the superstructure and the maxima of the PCDM are shown as dashed lines.

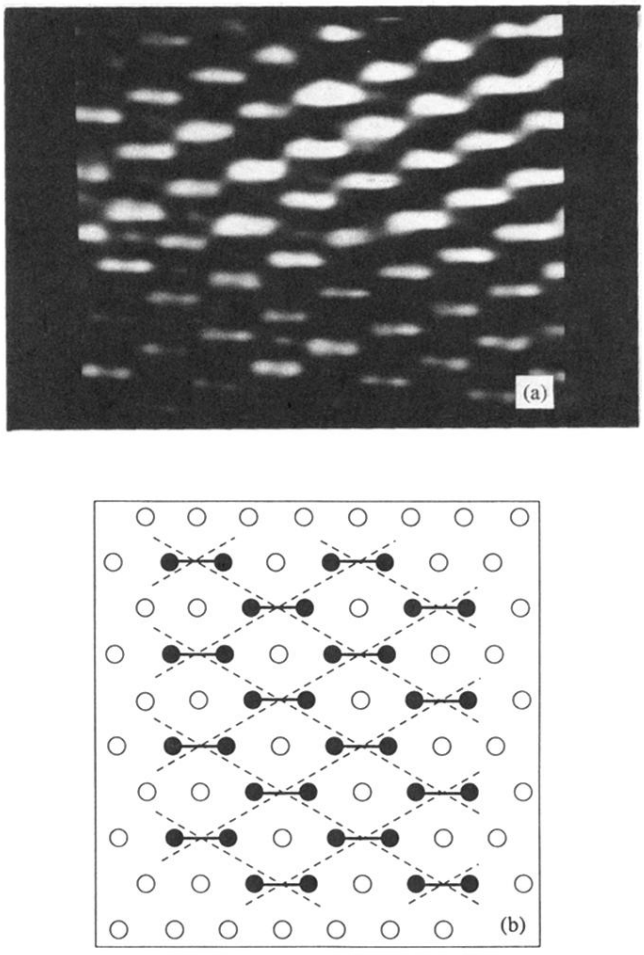

FIG. 3. (a) STM image of a superstructure with the PCDM's in two directions on the triangular graphite lattice. (b) Schematic model.

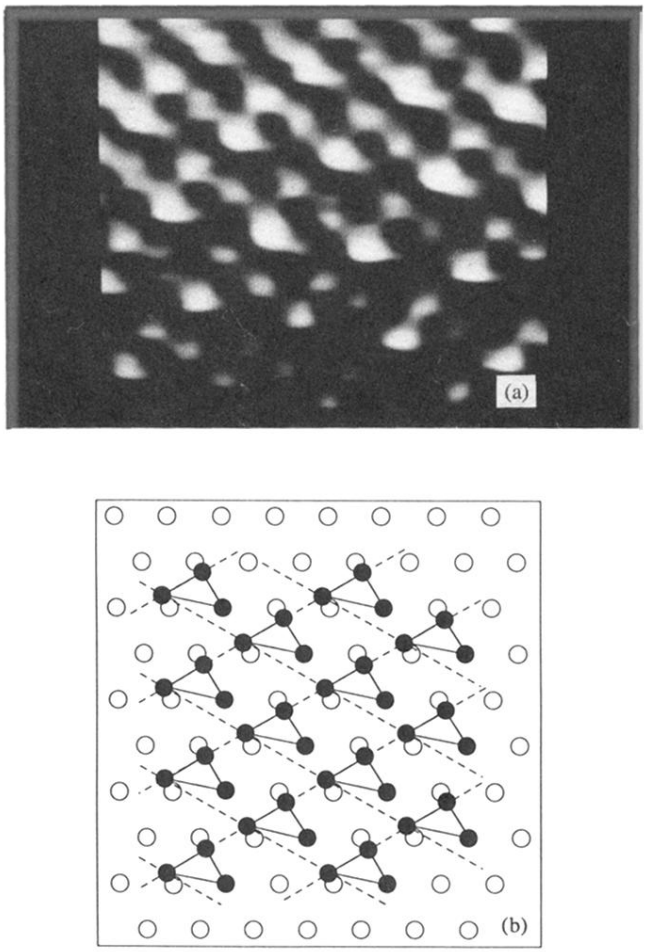

FIG. 4. (a) STM image of a superstructure with the PCDM's in two directions on the triangular graphite lattice but with different phases than in Fig. 3. (b) Schematic model.

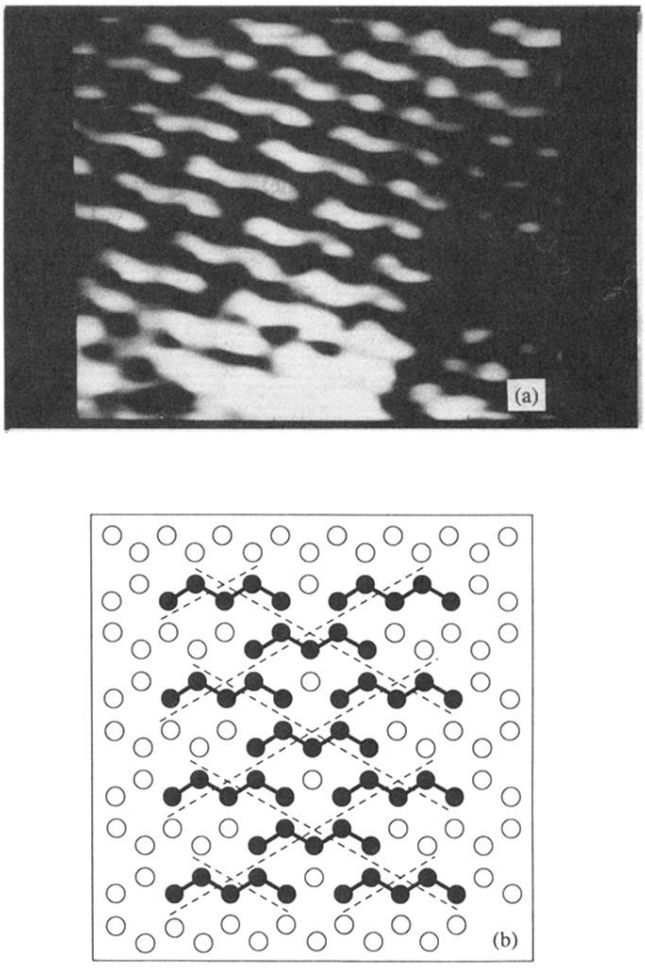

FIG. 5. (a) STM image of a superstructure with the PCDM's in two directions on the hexagonal graphite lattice. (b) Schematic model.

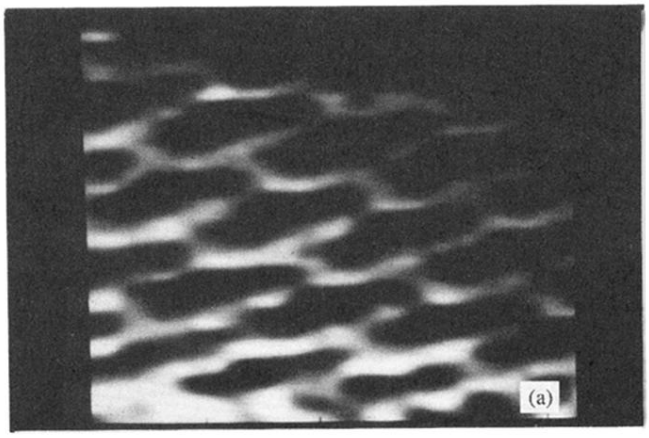

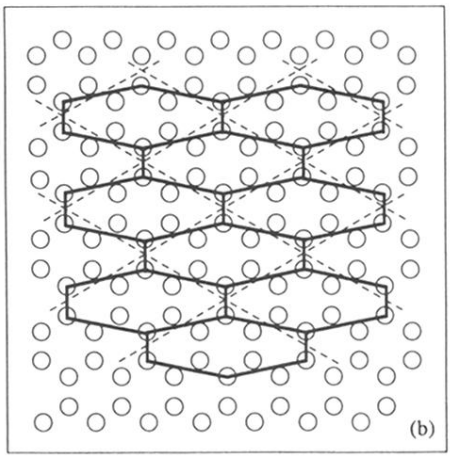

FIG. 6. (a) STM image of a superstructure with the PCDM's in two directions on the hexagonal graphite lattice but with different phases than in Fig. 5. (b) Schematic model.

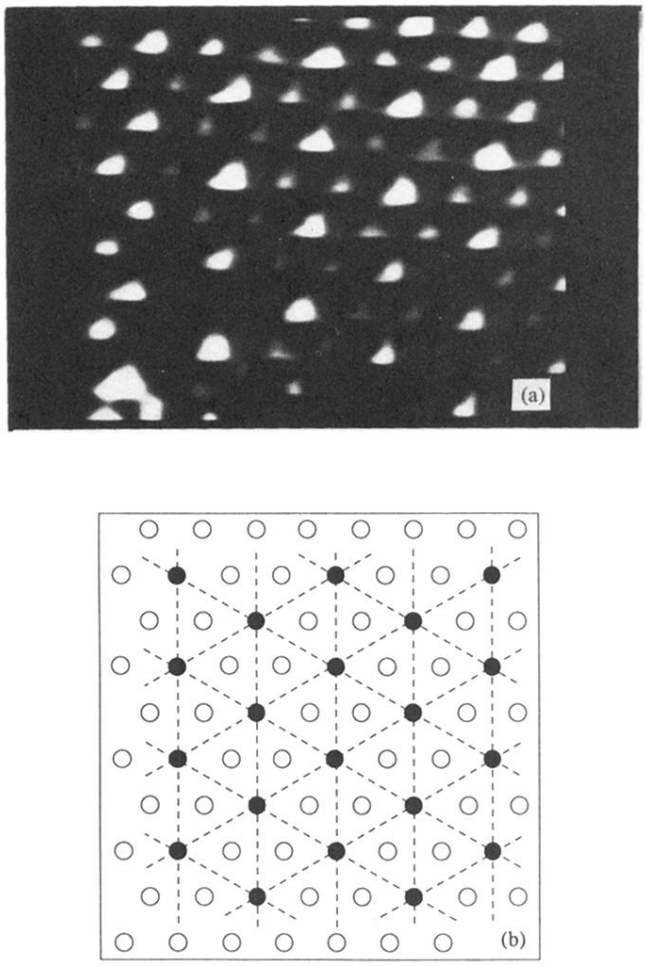

FIG. 7. (a) STM image of a superstructure with the PCDM's in three directions on the triangular graphite lattice. (b) Schematic model.

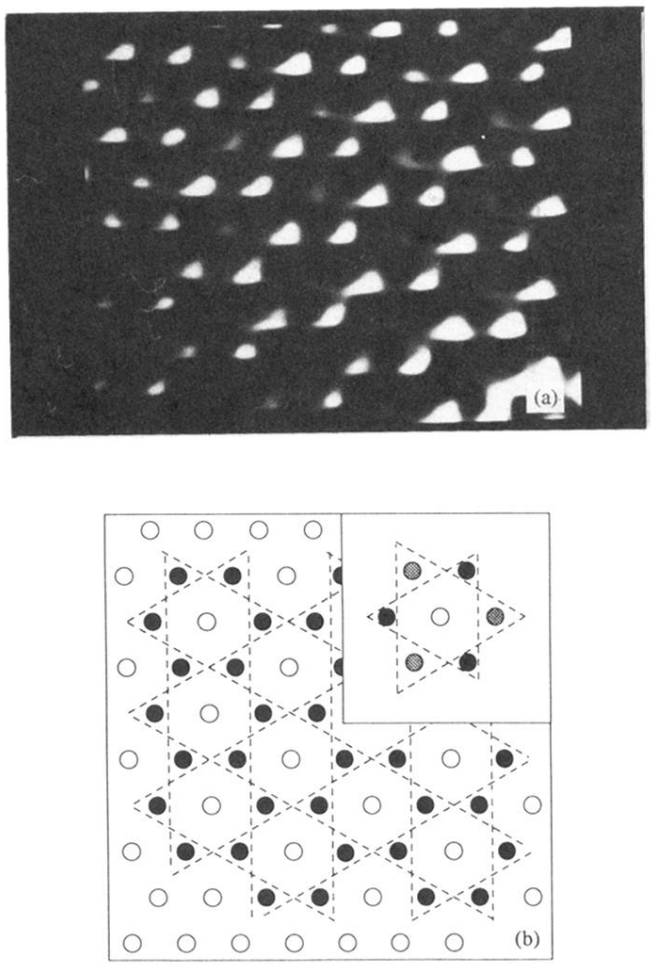

FIG. 8. (a) STM image of a superstructure with the PCDM's in three directions on the triangular graphite lattice but with different phases than in Fig. 7. (b) Schematic model. The inset shows the model of the brightness difference observed in (a).

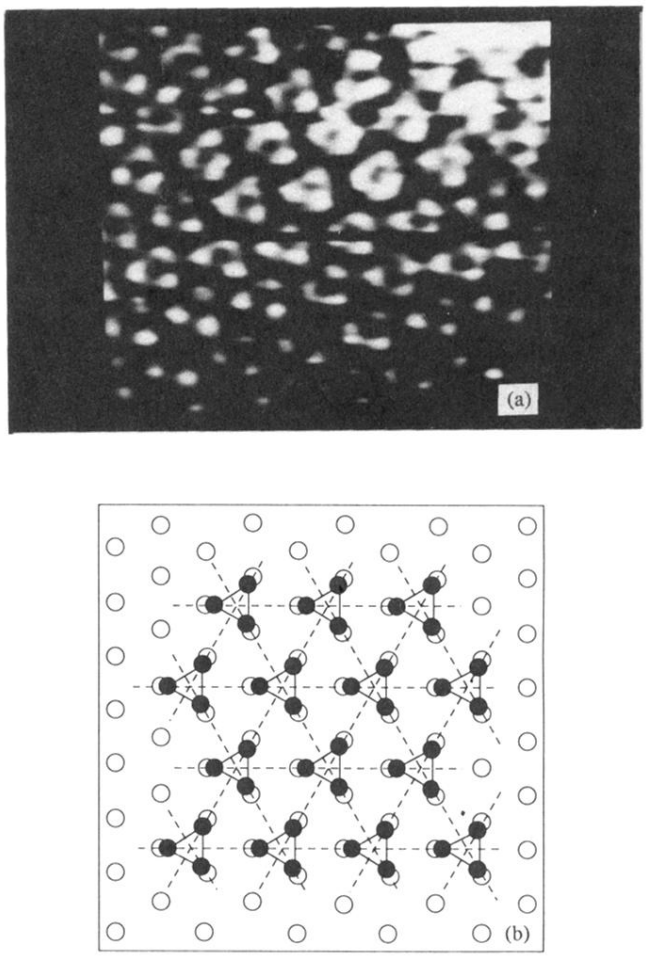

FIG. 9. (a) STM image of a superstructure with the PCDM's in three directions on the triangular graphite lattice but with different phases than in Figs. 7 and 8. (b) Schematic model.